Electroencephalography and clinical Neurophysiology, 1986, 63: 192–202
Elsevier Scientific Publishers Ireland, Ltd.

Technical Section

A NEW METHOD FOR ESTIMATION OF NERVE CONDUCTION VELOCITY DISTRIBUTION IN THE FREQUENCY DOMAIN [1]

GENJIRO HIROSE, YUGO TSUCHITANI * and JYONGSU HUANG *

*Department of Neurology, and * Central Clinical Laboratory, Kanazawa Medical University, Uchinada, Kahoku-gun, Ishikawa Pref. 920-02 (Japan)*

(Accepted for publication: July 1, 1985)

Summary Nerve conduction velocity (NCV) measurements have been widely used to assess the electrophysiological properties of peripheral nerves and to detect neuropathies at a subclinical stage. Conventional NCVs are usually expressed as the NCV for the fastest conducting fibers and the current standard methods do neither supply information about slower conducting fibers, nor detect information about individual fiber groups.

We present a new analytical method, to estimate the distribution of conduction velocity (DCV), based upon spectral analysis of the wave forms of two compound action potentials (CAPs) recorded by surface electrodes from a nerve bundle.

If the spectra of the two CAPs recorded at two different sites in response to supramaximal electrical stimulation at distances l_1 and l_2 are given as $G_{11}(\omega)$ and $G_{12}(\omega)$, the spectral representation of the latency distribution $P_{12}(\omega)$ for the propagation distance l_2 is expressed as follows:

$$P_{12}(l_1\omega/l_2) = \{G_{11}(\omega)/G_{12}(\omega)\}P_{12}(\omega),$$

where ω is an angular frequency.

We developed an algorithm that computes $P_{12}(\omega)$ successively without using iterative calculation methods.

Our estimation method is theoretically based upon the principle that the CAPs are recorded monopolarly to estimate the DCV, but in practical use, it is almost impossible to obtain appropriate CAP wave forms by monopolar recording methods, because of stimulation and muscle artefacts.

In order to evaluate the efficacy of bipolarly recorded CAP wave forms for this computation algorithm, we examined the two CAP wave forms reconstructed by simulation techniques. We found that the difference between the monopolar and bipolar recording methods was reflected in the wave form extracted for the single fiber action potentials but not in the latency distribution. The distance between the bipolarly recorded electrodes (1.5 cm was the minimal distance used) did not affect the reproducibility of estimating the latency distribution.

This new method is non-invasive and could be used for evaluation of peripheral neuropathies.

Keywords: *nerve conduction velocity distribution – compound action potential – single fiber action potential – frequency domain*

Nerve conduction velocity (NCV) measurements have been widely used to assess the electrophysiological function of peripheral nerves and to detect neuropathies at a subclinical stage. But conventional NCVs are usually expressed as the NCV for the fastest conducting fiber, and the current standard methods do not supply information about slower conducting fibers, nor do they detect information in individual fiber groups. A clinical method to assess the conduction characteristics of fiber groups in the nerve fiber bundle is really needed for the diagnosis and evaluation of peripheral neuropathy.

Gasser and Erlanger (1927), Hursh (1939) and others described the quantitative principles relating to nerve fiber diameter (FD), single-fiber action potential (SFAP), and nerve bundle compound action potential (CAP). The shape of the CAP is considered a function of 3 main variables: the distribution of conduction velocity (DCV), the distance between the stimulating and recording

[1] This work was supported by a grant from the Japanese Ministry of Education No. 58570366.

This paper was presented at the 7th International Congress of Electromyography, Munich, F.R.G., October 1983.

0013-4649/86/$03.50 © 1986 Elsevier Scientific Publishers Ireland, Ltd.

electrodes, and the shape of SFAPs. They have constructed CAPs based on the assumptions that the structure surrounding the nerve trunk is electrically linear, that the nerve fibers are all the same distance from the recording electrode, and that the fibers are electrically independent of each other.

They have also considered that the CAPs at a surface recording electrode could be expressed as a total sum of variously delayed individual SFAPs. The SFAP wave forms were modeled by a triangle which had the same propagation delays.

Recently Barker et al. (1979) and Cummins et al. (1979a,b) described a technique which measured the distribution of conduction velocity (CV) within the alpha fiber group, based upon the analysis of the shapes of two CAPs recorded by surface electrodes. Their methods analyzed two CAPs in the time domain. But their estimation method includes alternate calculations of velocity distribution and reference potentials until they converge to values which do not change significantly with further calculations by an iterative method. As they themselves (Barker et al. 1979) criticized the method, it is not possible to prove analytically whether their double conduction distance method is convergent or not and, in addition, there is no analytic proof that thus obtained results represent a unique solution to the problem.

This paper presents a new analytical method to estimate the distribution of CV by analyzing the relationship between CAP wave forms and the SFAP wave in the frequency domain. In this estimation we describe an algorithm that can be calculated sequentially without using iterative methods.

Estimation method for conduction velocity

(1) Formulation of the relationship between SFAP waves and CAP wave forms in the frequency domain

In order to formulate the relationship between SFAP and CAP, we have to assume the following processes. When a nerve trunk is electrically stimulated by a current pulse, each active fiber transmits a single impulse synchronously. As the impulse travels up the nerve trunk, it becomes desynchronized because of the different conduction velocities of the fiber groups. A surface electrode near the nerve detects a CAP formed by the sum of the SFAPs. The following 5 assumptions are necessary to formulate these processes.

(i) When a nerve trunk is transcutaneously stimulated by a short duration supramaximal pulse, each active nerve fiber evokes synchronously the same SFAP at the nearest site of the nerve trunk from the stimulated point. Each SFAP is elicited without any delay from the stimulation. We neglected the reduction of conduction distance due to any 'virtual cathode effect' (Wiederholt 1970).

(ii) The CV of the SFAP is constant between the sites of stimulation and recording, and a SFAP travels up a nerve with retention of the shape and amplitude.

(iii) All single nerve fibers in the nerve trunk are electrically independent of each other. And the transcutaneously obtained CAP is the sum of individual SFAPs that would be recorded if each fiber was stimulated separately.

Using the aforementioned assumptions, the CAP at the recording electrode at any time t with propagation delay for τ at a distance l may be expressed as follows (Fig. 1):

$$g_l(t) = \sum_{i-1}^{N} d_i(t - \tau_i) \qquad (1)$$

where gl(t) = the observed CAP as a function of time; N = the number of fiber classes; d_i = a function of the propagation delay for the fiber in class

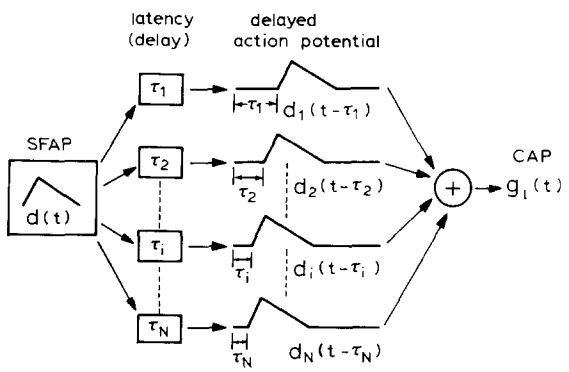

Fig. 1. Diagram of the CAP in terms of constituent SFAPs and their conduction characteristics. d(t), SFAP; τ_i, delay of the propagation time in CV class i; $d(t-\tau_i)$, delayed action potential at the delay τ_i.

i; and τ_i = the propagation delay for the fiber in class i at the distance l.

(iv) The number of active fibers N can be divided into M groups according to the delay value and if all the fibers in each group have the same SFAP, then eqn (1) is represented by

$$g_l(t) = \sum_{i=1}^{M} n_i d_i(t - \tau_i) \tag{2}$$

where n_i is the number of active fibers in each group, and then $N = \sum_{i=1}^{M} n_i$ is given.

(v) The duration and configuration of the SFAP are common in each fiber group which has the same fiber diameter, whereas the amplitude of the SFAP varies in each group. Thus $g_l(t)$ may be expressed as:

$$g_l(t) = \sum_{i=1}^{M} a_i \cdot n_i \cdot d(t - \tau_i) \tag{3}$$

where d(t) is a common factor of the SFAP in each group and a_i is the amplitude of the SFAP in the i group.

Then parameters a_i, n_i and τ_i are specific for the nerve fiber group, so $g_l(t)$ can be expressed using the parameter τ_i as follows:

$$g_l(t) = \sum_{i=1}^{M} p_l(\tau_i) d(t - \tau_i) \tag{4}$$

where $p_l(\tau_i)$ can be rewritten as $p_l(\tau_i)a_i \cdot n_i$. Furthermore eqn (4) can be expressed as a discrete formula after dividing it into M groups according to the delay value of τ_i. If τ_i is transformed into a continuous function using the continuous variable τ, the CAP can be expressed as

$$g_l(t) = \int_0^{\infty} p_l(\tau) d(t - \tau) d$$

$$= p_l(t) * d(t) \tag{5}$$

where * denotes the convolution operation.

Hence the CAP is expressed as a convolution in terms of the SFAP wave shape which is a common factor in each fiber group of the nerve fiber bundles and the latency distribution $p_l(\tau)$ for the propagation distance l along the nerve. Hence $p_l(\tau)$ is not a distribution of the number of nerve fibers, but of the amplitude spectrum of the CAP wave shape.

(2) The relationship between the two CAPs for the different distances of the stimulating and recording electrodes and the delay distribution

If a nerve trunk is stimulated at two different sites with different conduction distances, l_1 and l_2 ($l_1 > l_2$), then two CAP wave shapes can be obtained as follows:

$$g_{l1}(t) = p_{l1}(t) * d(t) \tag{6}$$

$$g_{l2}(t) = p_{l2}(t) * d(t) \tag{7}$$

Eqn (6) and (7) can be written via the FFT as follows.

$$G_{l1}(\omega) = P_{l1}(\omega) \cdot D(\omega)$$

$$G_{l2}(\omega) = P_{l2}(\omega) \cdot D(\omega)$$

where $G_{l1}(\omega)$, $G_{l2}(\omega)$, $P_{l1}(\omega)$, $P_{l2}(\omega)$, and $D(\omega)$ are the FFT of $g_{l1}(t)$, $g_{l2}(t)$, $p_{l1}(t)$, $p_{l2}(t)$ and d(t) respectively and $\omega(2\pi f)$ is an angular frequency.

The relationship between two CAP wave shapes is expressed in the frequency domain as follows.

$$G_{l1}(\omega)/G_{l2}(\omega) = P_{l1}(\omega)/P_{l2}(\omega) \tag{8}$$

In order to obtain the relationship between $p_{l1}(t)$ and $p_{l2}(t)$ when the CV of the i group is v_i, and the latencies for the distances l_1 and l_2 are τ_{i1} and τ_{i2} respectively, then $v_i = l_1/\tau_{i1} = l_2/\tau_{i2}$ is obtained where i = 1, 2, 3, ... M. Now as the distance between the stimulating and recording sites increases from l_1 to l_2, the bin width of the delay τ in each group increases by l_1/l_2 times on the histogram, thus the amplitude of each bin has to be reduced by l_2/l_1 times (Fig. 2a).

Fig. 2b is an illustration of an equivalent continuous function from eqn (5).

According to similar considerations as above, the CV is given by

$$v = l_1/\tau_i = l_2/\tau_2 \tag{9}$$

For the very short distance $\Delta\tau$ of $p_{l1}(\tau)$,

$$p_{l1}(\tau_1) \cdot \Delta\tau = p_{l2}(\tau_2) \cdot \frac{l_2}{l_1} \Delta\tau \tag{10}$$

and

$$\int_0^{\infty} p_{l1}(\tau) d\tau = \int_0^{\infty} p_{l2}(\tau) d\tau$$

The correlation between the two latency distribu-

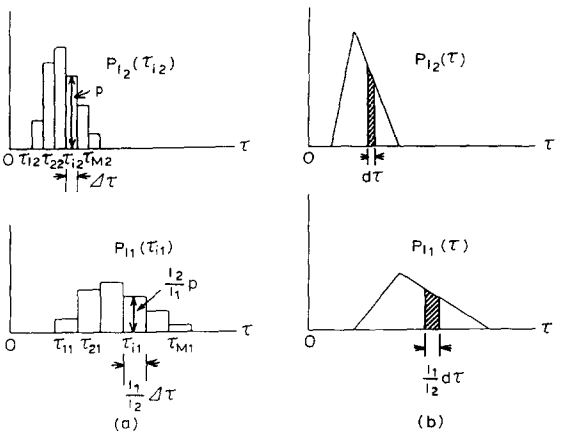

Fig. 2. Diagrammatic representation of two latency distributions for two different conduction distances where the distance l_1 is equal to $2l_2$. a: discrete functions of the two latency distributions, $p_{12}(\tau)$ and $p_{11}(\tau)$. b: continuous functions of the two latency distributions.

tions is given from eqn (9) and (10) as follows:

$$\frac{l_1}{l_2}p_{11}(\tau) = p_{12}\left(\frac{l_2}{l_1}\tau\right) \tag{11}$$

via Fourier transforming, eqn (11) becomes

$$P_{11}(\omega) = P_{12}\left(\frac{l_1}{l_2}\omega\right) \tag{12}$$

Here substituting eqn (8) into eqn (12) gives us the following:

$$p_{12}\left(\frac{l_1}{l_2}\omega\right) = \{G_{11}(\omega)/G_{12}(\omega)\}P_{12}(\omega) \tag{13}$$

Hence, the correlation between the latency distribution for the distance l_2 and two CAPs is represented by a formula in the frequency domain.

(3) Computational algorithm for $P_{12}(\omega)$

If the value of $P_{12}(\omega)$ is given at $\omega = \omega_0$, $P_{12}\{(l_1/l_2)\omega_0\}$ is estimated by using eqn (13), then $P_{12}\{(l_1/l_2)^2\omega_0\}$, and $P_{12}\{(l_1/l_2)^3\omega_0\}$, ... are estimated as higher frequency components successively.

In practice, $g_{11}(t)$ and $g_{12}(t)$ are uniformly sampled to get N absolute values, $g_{11}(nT)$ and $g_{12}(nT)$ where T is the sampling interval and n is the sample number. Then $G_{11}(\omega)$ and $G_{12}(\omega)$ are given by the discrete Fourier transforms as

$$G_{11}(k\Omega) = \sum_{n=0}^{N-1} g_{11}(nT)e^{-jnTk\Omega}$$

$$G_{12}(k\Omega) = \sum_{n=0}^{N-1} g_{12}(nT)e^{-jnTk\Omega}$$

where $k = 0, 1, 2, \ldots, N-1$ (integer). N = the transform points of the discrete Fourier transform; T = the sampling interval (sec) in the time domain; $\Omega(1/NT)$ = the sampling interval (Hz) in the frequency domain.

In order to estimate $P_{12}(\omega)$ for equally spaced values of frequency, $\omega = k$ ($k = 0, 1, 2, 3, \ldots, N = 1$), eqn (13) will be transformed into a more convenient form.

$$P_{12}\left(\frac{l_1}{l_2}k\Omega\right) = G(k\Omega)\cdot P_{12}(k\Omega)$$

but $G(k\Omega) = G_{11}(k\Omega)/G_{12}(k\Omega)$.

Then, by setting $a = l_1/l_2$, the above equation becomes:

$$P_{12}(k\Omega) = G(k\Omega/a)\cdot P_{12}(k\Omega/a) \tag{14}$$

Here $G(k\Omega/a)$ and $P_{12}(k\Omega/a)$ can be calculated by linear interpolation between $G([k/a]\Omega)$ and $G([k/a+1]\Omega)$, $P_{12}([k/a]\Omega)$ and $P_{12}([k/a+1]\Omega)$ respectively (but [x] is an integer part of X), then the amplitude and phase spectra of $P_{12}(k\Omega)$ can be given as follows:

$$\begin{aligned}|P_{12}(k\Omega)| = A(k\Omega)\cdot\big[\{\,&|P_{12}([k/a+1]\Omega)| \\ &-|P_{12}([k/a]\Omega)|\}\cdot(k\Omega/a-[k/a]\Omega) \\ &+|P_{12}([k/a]\Omega)|\big]\end{aligned} \tag{15}$$

$$\begin{aligned}\arg\{P_{12}(k\Omega)\} = B(k\Omega) &+ [\arg\{P_{12}([k/a+1]\Omega)\}] \\ &- \arg\{P_{12}([k/a]\Omega)\} \\ &\cdot(k\Omega/a-[k/a]\Omega) \\ &+ \arg\{P_{12}([k/a]\Omega)\}\end{aligned} \tag{16}$$

where $A(k\Omega) = \{\,|G([k/a+1]\Omega)| - |G([k/a]\Omega)|\}\cdot(k\Omega/a-[k/a]\Omega) + |G([k/a]\Omega)|$

$B(k\Omega) = \arg\{G([k/a+1]\Omega)\} - \arg\{G([k/a]\Omega)\}\cdot(k\Omega/a-[k/a]\Omega) + \arg\{G([k/a]\Omega)\}$.

By setting $|P_{12}(1)| = 1$, $\arg\{P_{12}(0\cdot\Omega)\} = 0$ as initial conditions, where $a > 1$, $|P_{12}(k\Omega)|$, $\arg\{P_{12}(k\Omega)\}$ can be given successively from the lower frequency components. But the solution of the lower frequency component is dependent upon the value of a as follows.

(I) When $a > 2$

Substitution 1 for k in eqn (15) and (16), then each equation will be expressed as follows,

$$|P_{12}(0 \cdot \Omega)| = \{1/A(\Omega) - \Omega/a\}/(1 - \Omega/a) \quad (17)$$

$$\arg\{P_{12}(1 \cdot \Omega)\} = B(\Omega)/(1 - \Omega/a) \quad (18)$$

(II) When $\frac{3}{2} < a \leqslant 2$

$|P_{12}(0 \cdot \Omega)|$ and $\arg\{P_{12}(1 \cdot \Omega)\}$ can be given from eqn (17) and (18) respectively and putting $k = 2$ into eqn (15) and (16), then each equation will be expressed as follows.

$$|P_{12}(2\Omega)| = (1 - 2\Omega/a + \Omega)/\{1/A(2\Omega) - 2\Omega/a + \Omega\} \quad (19)$$

$$\arg\{P_{12}(2\Omega)\} = B(2\Omega)/(1 - 2\Omega/a + \Omega) + \arg\{P_{12}(\Omega)\} \quad (20)$$

(III) When $\frac{4}{3} < a \leqslant \frac{3}{2}$

$|P_{12}(0 \cdot \Omega)|$, $\mathrm{Arg}\{P_{12}(1 \cdot \Omega)\}$, $|P_{12}(2\Omega)|$ and $\arg\{P_{12}(2\Omega)\}$ can be given from eqn (17), (18), (19) and (20) respectively. And substituting 3 for k in eqn (15) and (16), then,

$$|P_{12}(3\Omega)| = [(1 - 3\Omega/a + 2\Omega)/\{1/A(3\Omega) - 3\Omega/a + 2\Omega\}] \cdot |P_{12}(2\Omega)|$$

$$\arg\{P_{12}(3\Omega)\} = B(3\Omega)/(1 - 3\Omega/a + 2\Omega) + \arg\{P_{12}(2\Omega)\}$$

Here, as the value of a becomes closer to 1, namely the two CAP wave forms become more similar in configuration, so that the numbers of the lower frequency components which should be obtained separately increase more.

Via the inverse FFT of $P_{12}(k\Omega)$, $p_{12}(t)$ can be given at the distance l_2 between the stimulating and recording sites, so the DCV can be estimated. And eqn (7) can be rewritten via the FFT as follows.

$$D(\omega) = G_{12}(\omega)/P_{12}(\omega)$$

From this equation, the SFAP wave form d(t) can be estimated.

Subjects and application of the method

Informed consent was obtained from 10 healthy young individuals from 21 to 32 years old. In order to reduce arm movement artefacts, the forearm and the hand were fixed to a splint in the region illustrated by the broken lines in Fig. 3.

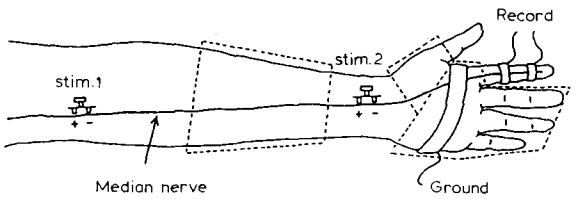

Fig. 3. Recording method the 2 CAPs from a median nerve. The broken lines indicate areas of fixation to the arm-board.

Median nerve CAPs were recorded bipolarly by the ring electrode from the 2nd finger in response to supramaximal electrical stimulation at the elbow and wrist (Fig. 3). The recorded CAPs were amplified by a DISA evoked response EMG system (bandwidth 2 Hz–2 kHz) and the final wave form was the average of 20 stimuli. The stimulus was a monophasic square-wave current (0.2 msec duration) at a rate of 1/sec. The CAP wave forms were digitized (512 points) with a sample time of 25 msec and stored on cassette discs. The application method is shown in Fig. 4. Data analysis was

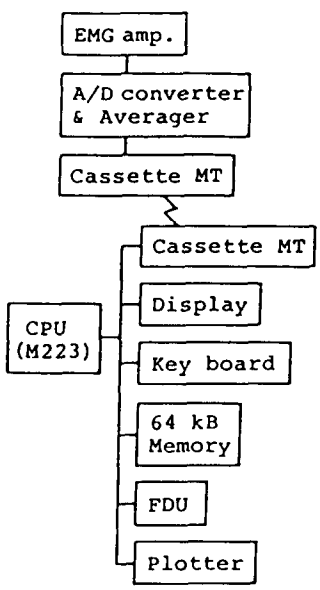

Fig. 4. Diagram of the system for the estimation of DCVs. EMG amp., electromyogram amplifier; CPU, central processing unit; FDU, floppy disk unit.

done by a microcomputer, Sord M223-V (memory capacity 64KB), using BASIC language programs.

Data analysis procedures

The flow chart of the CAP analysis procedures is shown in Fig. 5. The recorded double CAPs (Fig. 6a) were pretreated in the form of dialogue to remove artefacts such as stimulus tails and muscle movements, to make a smoothing of the wave forms by obtaining the moving average from near 3 points and to set the interval between the stimulus and the starting point of the CAPs to a zero level.

The propagation delays of the zero signal components in the CAPs were removed in order to minimize the error of processing the phase component after FFT (Fig. 6b). The CAP wave forms were transformed to spectra and separated into magnitude and phase components. Fig. 7a illustrates the magnitude spectra of the Fourier

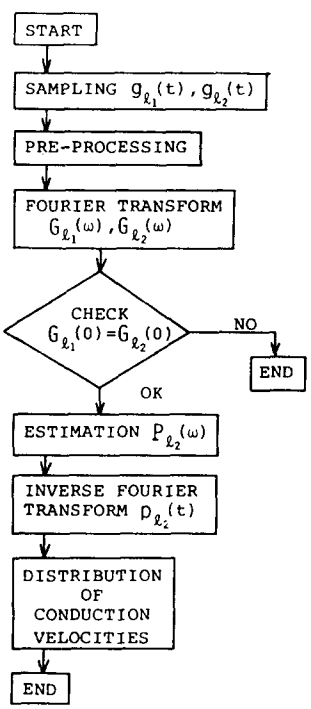

Fig. 5. The flow chart of on-line data processing of the estimation of DCVs.

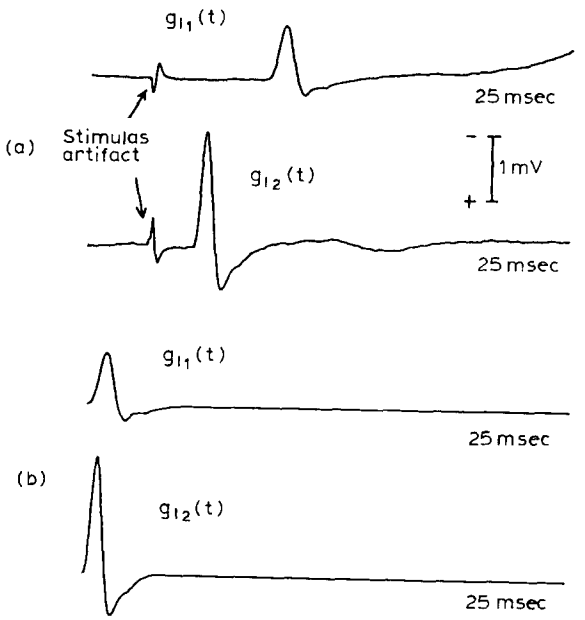

Fig. 6. Examples of two CAP wave forms. a: actual tracings of CAPs before processing. b: reconstructed tracings of CAPs after processing.

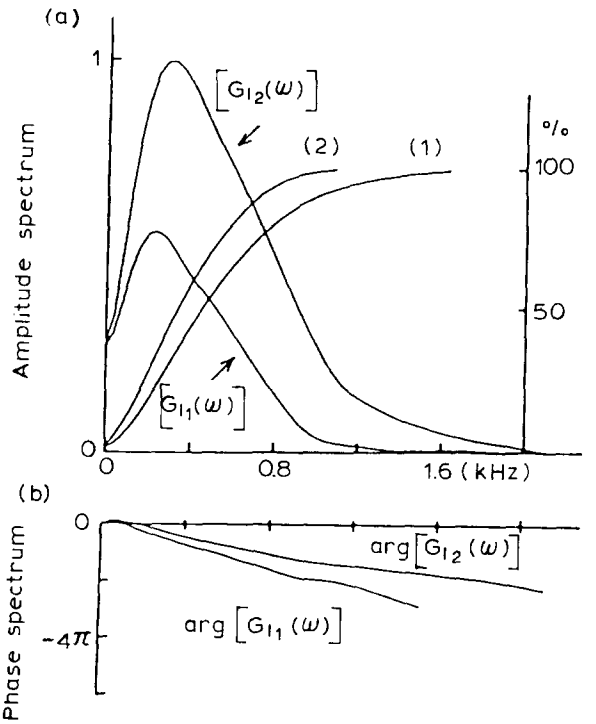

Fig. 7. Spectral representation of the two CAPs. a: amplitude spectrum. 1, cumulative distribution of $|G_{l2}(\omega)|$; 2, cumulative distribution of $|G_{l1}(\omega)|$. b: phase spectrum.

transformed CAP wave forms and the normalized cumulative frequency distributions. The phase spectra obtained by the FFT were principal values and discontinuous, so the appropriate integer power of 2π was added to satisfy the continuity in the phase curves (Fig. 7b; Oppenheim and Schafer 1975).

When substituting 0 for ω in eqn (13), then $G_{11}(0) = G_{12}(0)$ is obtained, and the zero signal components for the amplitude spectrum of the two CAPs have to be exactly the same. Therefore, by way of the estimation, we can check whether the DCVs can be estimated from the two CAPs. In a practical calculation, if the error of the zero signal components of the amplitude spectrum from the two CAPs was less than 20%, we considered them appropriate for further analysis and were able to estimate DCVs.

Then $P_{12}(\omega)$ is calculated according to the preceding estimation algorithm. $P_{12}(\omega)$ has a low S/N value in the higher frequency region, so that cosine tapering (Bendat and Piersol 1971) is applied to the higher frequency components of the absolute value of $P_{12}(\omega)$.

The latency distribution $p_{12}(t)$ is obtained via the inverse FFT by replacing the real part and the imaginary part of $P_{12}(\omega)$ as their even and odd functions respectively (Fig. 8a).

The DCVs calculated from $p_{12}(t)$ and the conduction distance l_2 are expressed with a bin width of 1 m/sec as the abscissa (Fig. 8b).

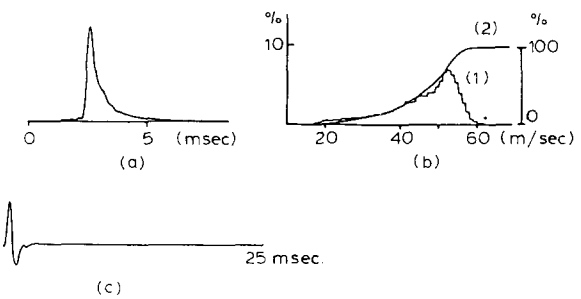

Fig. 8. Examples of the latency distribution, DCV and SFAP wave form in a normal individual. a: latency distribution. b: distribution of the conduction velocity (1) and its cumulative distribution (2). The small dot indicates the value of the maximal NCV determined by conventional methods. c: SFAP wave form.

The SFAP wave form is expressed after normalization of the negative peak value (Fig. 8c).

Study on the estimation accuracy using simulated CAP wave forms

(1) Simulation method of CAP wave forms

By assuming the monopolarly recorded SFAP wave forms and the DCVs, the latency distributions are calculated at the conduction distances of 35 cm and 14 cm. Then we simulated the two monopolarly recorded CAPs (Fig. 9a). We used a triphasic wave form similar to the one which Buchthal and Rosenfalck (1966) used and a double peaked distribution curve from a healthy individual for an assumed monopolarly recorded SFAP wave form and a DCV respectively.

As for a bipolarly recorded CAP wave form, we first found the two monopolarly recorded CAPs at the conduction distance of 1 and $1+\alpha$ with a distance between bipolar electrodes as α and we simulated the wave form as the difference between them (Fig. 9b; Buchthal and Rosenfalck 1966).

We applied our estimation method for these simulated wave forms and evaluated how the dif-

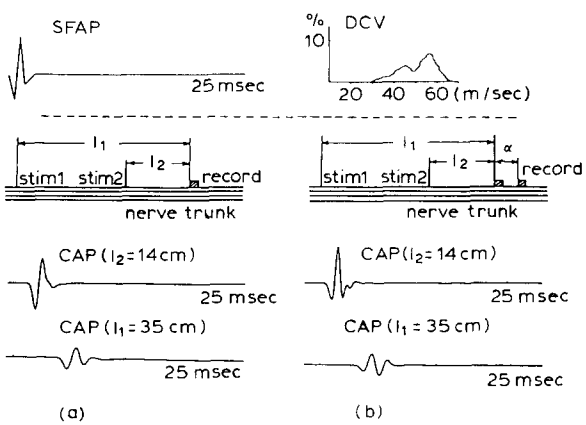

Fig. 9. Simulation of monopolarly and bipolarly recorded CAP models. a: the top part illustrates SFAP from a simulation model at l_1 (35 cm) and l_2 (14 cm) distances between the stimulation and recording sites. The bottom part shows the simulated CAPs. b: the top illustrates DCV from a model at l_1 and l_2 distance between the stimulation and recording sites. α indicates a distance between the recording electrodes. The bottom part shows the simulated CAPs.

ferent estimation methods of CAPs influence the obtained DCV and SFAP wave forms.

(2) Results of the simulated CAP wave forms

Fig. 10a illustrates the DCV and SFAP wave forms, estimated from the monopolarly reconstructed CAP wave forms. The estimated DCV is shifted by 1.2–2.2 m/sec toward the lower conduction velocities from the original DCV at the points of 15, 50 and 90% of the accumulation distribution, and the peak value of the DCV is also shifted by 3 m/sec toward the lower conduction velocities. On the whole, the estimated DCV is shifted toward the lower CV side, but coincides well with the original DCV in its configuration. The estimated SFAP also coincides with the original wave form.

The DCV estimated from the bipolarly recorded CAPs at the distance between the recording electrodes = 2 cm, is shifted by 1.3–2.9 m/sec toward the lower CV side at the point of 15, 50 and 90% of the accumulation distribution, and the peak value of the DCV is shifted by 3 m/sec toward the lower CV side, but the whole distribution coincides with the original one. A similar tendency is seen regardless the change of the distance between the electrodes at 1.5 and 3 cm. But the estimated SFAP wave form is different from the monopolarly recorded original wave form and varies according to the distance between the recording electrodes (Fig. 10b, c and d). So the estimated DCV is generally not influenced by the change of recording conditions of CAPs, whereas the estimated SFAP is greatly influenced by the change of such conditions.

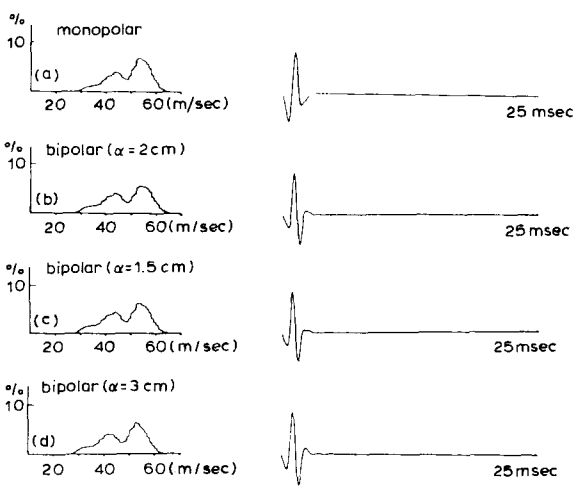

Fig. 10. DCVs and SFAP wave forms predicted by the simulation model. a: monopolarly recorded model. b: bipolarly recorded model with the distance $\alpha = 2$ cm between the recording electrodes. c: bipolarly recorded model with the distance $\alpha = 1.5$ cm between the recording electrodes. d: bipolarly recorded model with the distance $\alpha = 3$ cm between the recording electrodes.

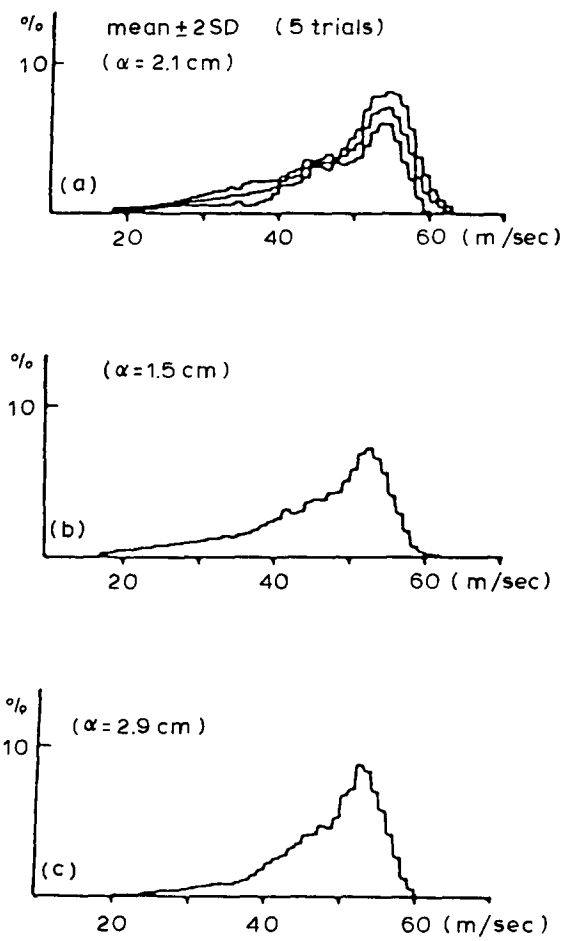

Fig. 11. Reproducibility of estimated DCVs. a: $\alpha = 2.1$ cm. 3 DCVs indicate the mean ± 2 S.D. values in 5 trials. b: $\alpha = 1.5$ cm. c: $\alpha = 2.9$ cm.

Results of clinical application

(1) Reproducibility

The DCVs from a healthy individual were estimated by our method, using bipolar recording electrodes with separation distances of 2.1, 1.5, and 2.9 cm. At 2.1 cm, the mean value ± 2 S.D.s from 5 trials is illustrated in Fig. 11a. The S.D. of the DCV from 5 trials is almost constant at each CV and the coefficient of variation is 20.6% between 25 and 40 m/sec and 7.7% between 40 and 55 m/sec. And the mean velocity ± 2 S.D.s at the peak of the DCV is 53.4 ± 0.9 m/sec and the mean values ± 2 S.D.s at the point of 15%, 50% and 90% of the accumulation distribution are 37.8 ± 1.9 m/sec, 50.1 ± 0.8 m/sec and 56.8 ± 0.7 m/sec, respectively, and they show good reproducibility.

At 1.5 and 2.9 cm separation distance, the estimated velocities vary within 3.3 m/sec at the point of each percentage in their estimated distributions (Fig. 11b and c). It seems that the variation of the separation distance between bipolar recording electrodes does not affect the DCV significantly.

The DCVs for 10 healthy individuals fell between 20 and 65 m/sec with the peak value of the DCV between 52 and 60 m/sec, and the value of the conduction velocity measured by a conventional method is illustrated as a black dot in each distribution of Fig. 12. They are quite similar to the value of the maximal conduction velocity determined by our new method.

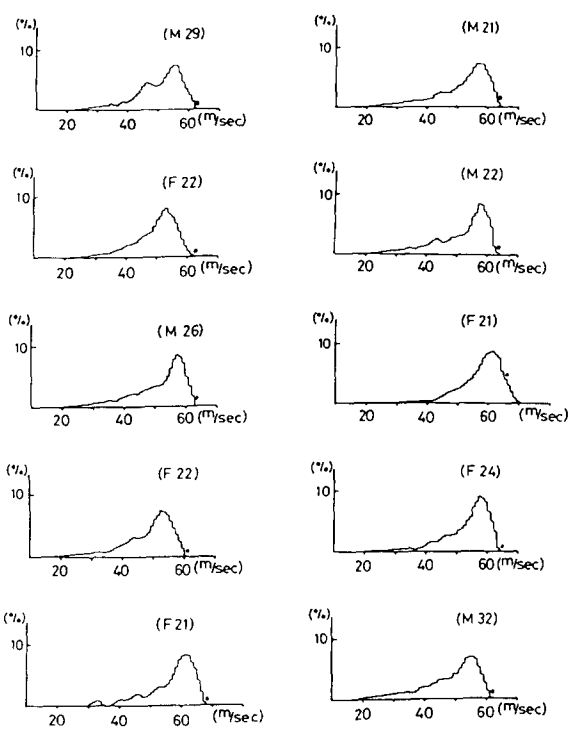

Fig. 12. Calculated median nerve DCVs from 10 normal healthy individuals. M, male; F, female; number indicates the age of the individual. The black dot in each DCV indicates the value of the maximal NCV by conventional methods.

Discussion

Barker et al. (1979) and Cummins et al. (1979a, b) have already proposed the new analytic methods for the estimation of DCVs in the time domain by using 2 CAPs recorded from 2 different sites with different distances between the stimulating and recording electrodes. But their estimation method consists of the successive approximation method. In their method it is not possible to prove whether their answers are convergent and there is also no evidence that their calculated results yield a unique solution to the problem

On the other hand, our method has advantages that we can estimate the spectrum component of the latency distribution in a short time and in a unique way by using the spectrum ratio of the two CAP wave forms. But the method of Barker et al. (1979) has the constraint that all the solutions must be positive or zero, whereas in our method there is no such guarantee of the positivity of DCV and, in fact, we had some cases where the DCVs had negative solutions when the two CAPs had different zero signal components of the amplitude spectrum (the mean value of each signal). As we mentioned earlier, if the difference between the zero signal components in the amplitude spectrum of two CAPs is less than 20%, then we are able to obtain positive DCVs, and we can check those zero signal components of CAPs on the way of estimation.

The assumptions on electrical impulse propa-

gation within nerve fibers, which were used in our estimation method, are basically the same as those Barker et al. (1979) and Cummins et al. (1979a, b) used in their methods. In regard to the duration of SFAPs, BeMent (1981) reported that the SFAP duration decreases as the CV increases and the variations in SFAP duration are less than 0.1 msec (Paintal 1966; BeMent 1981) when CVs are between 20 and 80 m/sec. So the duration variations are considered insignificant over the range (35–80 m/sec) of CVs studied in our method.

In our method, CAPs were recorded bipolarly from the index finger at the distal part of the PMP joint in response to two sites of stimulation at the wrist and elbow. In this methodology, the median nerve is stimulated proximally to the recording site, and the CAPs are obtained from the same site distally. Therefore the two CAPs consist of the summation of SFAPs from the same fibers activated at the two sites. Under these conditions, the variation of each CAP reflects only the variations of the latency distributions.

Whereas in the method of Barker et al. (1979), CAPs were recorded monopolarly from the axilla in response to stimulation at the wrist and elbow so that this technique has the disadvantage that the populations of stimulated nerve fibers differ at the two stimulation sites because of branching of a median nerve between the wrist and elbow, the fiber constituents of his two CAPs differ. On the other hand, Cummins et al. (1979a,b) used the method where CAPs were recorded monopolarly from the median nerve at the elbow and axilla, in response to stimulation at the wrist. In their method the same populations of fibers were stimulated at the two different sites, so that the CAPs obtained consist of the summation of the same population of SFAPs. However, the distance between the surface recording electrode and the nerve fiber bundle differs significantly between the axilla and elbow, and they should have accounted for the different distances in their approach. We tried Barker's and Cummins' methods with monopolar recording electrodes, but the muscle movement artefacts after supramaximal stimulation interfered with our ability to record reasonable CAPs by their methods. Because of these difficulties we chose the bipolar recording method. From our simulation studies of monopolarly and bipolarly obtained CAPs, we conclude that we can get accurate estimations of DCV from the bipolar recording method.

Our method is unique because the method of Cummins et al. (1979a) calculated the DCVs in the time domain, where the process of obtaining the convergence of CV was needed by iterative calculations, whereas our method calculates the DCVs in the frequency domain after the FFT of CAPs where only multiplication is needed without iterative calculations.

The advantages of DCVs obtained by our method are that it is non-invasive, less time consuming than histological studies, and can be used in serial studies to follow the evolution of peripheral nerve dysfunctions or the progress of dysfunction remedies.

This new approach may not be a substitute for the histological fiber diameter distribution but an addendum or alternative electrophysiological measurement to obtain peripheral nerve fiber populations.

Résumé

Une nouvelle méthode pour estimer la distribution de la vitesse de conduction nerveuse dans le domaine fréquentiel

La mesure de la vitesse de conduction nerveuse est un moyen largement employé pour déterminer les propriétés électrophysiologiques des nerfs périphériques et pour détecter des neuropathies avant l'apparition des symptômes cliniques. Les mesures habituelles sont le plus souvent exprimées en fonction de la vitesse des fibres les plus rapides et les méthodes standard courantes n'apportent pas d'informations sur les fibres plus lentes, ou sur les groupes individuels de fibres.

Nous présentons une nouvelle méthode d'analyse pour estimer la distribution des vitesses de conduction (DVC), basée sur l'analyse spectrale des formes d'ondes de deux potentiels d'action complexes (PAC) enregistrés par des électrodes de surface sur un faisceau de fibres.

Si, en réponse à la stimulation électrique

supramaximale, les spectres des deux PAC — $G_{l1}(\omega)$ et $G_{l2}(\omega)$ — sont enregistrés en deux sites distincts à des distances l_1 et l_2, la représentation spectrale de la distribution des latences $P_{l2}(\omega)$ pour la distance de propagation l_2 est exprimée par:

$$P_{l2}(l_1\omega/l_2) = \{G_{l1}(\omega)/G_{l2}(\omega)\}P_{l2}(\omega),$$

où ω représente la fréquence angulaire.

Nous avons mis au point un algorithme qui calcule $P_{l2}(\omega)$ successivement sans utiliser de méthode de calcul itératif.

Notre méthode d'estimation est théoriquement basée sur le principle que les PAC sont enregistrés en monopolaire pour estimer la DVC; en pratique cependant, il est presque impossible d'obtenir des formes d'onde de PAC appropriées en utilisant un tel enregistrement en raison des artéfacts de stimulation et des artéfacts musculaires.

Afin d'évaluer l'efficacité d'enregistrements bipolaires des formes d'ondes des PAC, pour le calcul de cet algorithme, nous avons étudié les formes d'onde de deux PAC reconstruits par des techniques de simulation. Nous avons trouvé que la différence entre enregistrements bipolaire et monopolaire était reflétée dans la forme d'onde obtenue pour les potentiels d'action d'une fibre isolée, mais non dans la distribution des latences. La distance entre les électrodes d'enregistrement bipolaire (1,5 cm était la distance minimale utilisée) n'a pas affecté la reproductibilité des estimations de distributions des latences.

Cette nouvelle méthode est non-invasive et peut être utilisée pour l'estimation des neuropathies périphériques.

We gratefully acknowledge the preparation of the manuscript by Miss Kazuko Shikada and the cooperation of our healthy volunteers.

References

Barker, A.T., Brown, B.H. and Freeston, I.L. Determination of the distribution of conduction velocities in human nerve trunks. IEEE Trans. Biomed. Engng, 1979, BME 26: 76–81.

BeMent, S.L. Single myelinated peripheral nerve fibers. Anatomic and electrophysiologic studies relevant to conduction velocity and fiber diameter histogram prediction from surface recorded potentials. In: L.J. Dorfman, K.L. Cummins and L.J. Leifer (Eds.), Conduction Velocity Distributions, a Population Approach to Electrophysiology of Nerve. Alan R. Liss, New York, 1981: 33–55.

Bendat, J.S. and Piersol, A.G. Random Data: Analysis and Measurement. Wiley-Interscience, New York, 1971: 323–325.

Buchthal, F. and Rosenfalck, A. Evoked action potentials and conduction velocity in human sensory nerves. Brain Res., 1966, 3: 1–122.

Cummins, K.L., Perkel, D.H. and Dorfman, L.J. Nerve fiber conduction-velocity distributions. I. Estimation based on the single-fiber and compound action potentials. Electroenceph. clin. Neurophysiol., 1979a, 46: 634–646.

Cummins, K.L., Dorfman, L.J. and Perkel, D.H. Nerve fiber conduction-velocity distribution. II. Estimation based on two compound action potentials. Electroenceph. clin. Neurophysiol., 1979b, 46: 647–658.

Gasser, H.S. and Erlanger, J. The role played by the sizes of constituent fibers of the nerve trunk in determining the form of its action potential wave. Amer. J. Physiol., 1927, 80: 522–545.

Hursh, J.B. Conduction velocity and diameter of nerve fibers. Amer. J. Physiol., 1939, 127: 131–139.

Oppenheim, A.V. and Schafer, R.W. Digital Signal Processing. Prentice-Hall, Englewood Cliffs, NJ, 1975: 496–497.

Paintal, A.S. The influence of diameter of medullated nerve fibres of cats on the rising and falling phases of the spike and its recovery. J. Physiol. (Lond.), 1966, 184: 791–811.

Wiederholt, W.C. Stimulus intensity and site of excitation in human median nerve sensory fibers. J. Neurol. Neurosurg. Psychiat., 1970, 33: 438–441.